Adaptive X-ray Optics Development at AOA-Xinetics

Charles F. Lillie*[a], Jeffrey L. Cavaco[b], Audrey D. Brooks[b],
Kevin Ezzo[b], David D. Pearson[c] , John A. Wellman[d]
[a]Lillie Consulting LLC, 6202 Vista del Mar, Playa del Rey, CA, USA 90293-8802;
[b]Northrop Grumman AOA-Xinetics, 115 Jackson Road, Devens, MA USA 01434
[c]Dynapeiron, 3 Forbes Road, Hudson, MA 01749
[d]Metenco LLC, 5 Montview Road, Chelmsford, MA 01824

ABSTRACT

Grazing-incidence optics for X-ray applications require extremely smooth surfaces with precise mirror figures to provide well focused beams and small image spot sizes for astronomical telescopes and laboratory test facilities. The required precision has traditionally been achieved by time-consuming grinding and polishing of thick substrates with frequent pauses for precise metrology to check the mirror figure. More recently, substrates with high quality surface finish and figures have become available at reasonable cost, and techniques have been developed to mechanically adjust the figure of these traditionally polished substrates for ground-based applications. The beam-bending techniques currently in use are mechanically complex, however, with little control over mid-spatial frequency errors. AOA-Xinetics has been developing been developing techniques for shaping grazing incidence optics with surface-normal and surface-parallel electrostrictive Lead magnesium niobate (PMN) actuators bonded to mirror substrates for several years. These actuators are highly reliable; exhibit little to no hysteresis, aging or creep; and can be closely spaced to correct low and mid-spatial frequency errors in a compact package. In this paper we discuss recent development of adaptive x-ray optics at AOA-Xinetics.

Keywords: Deformable mirrors, grazing incidence optics, bendable mirrors, X-ray telescopes, adaptive optics

1. INTRODUCTION

AOA-Xinetics has been focused on advancing the state of the art of active optics for more than 20 years by improving and maturing conventional actuator and DM technology, by inventing new architectures with unique characteristics to expand DM performance and applicability, and by applying actuator and DM technology to new applications to enable game changing optical systems.

Adaptive optics had its origins in the 1970's with the development of deformable mirrors (DMs) to compensate for atmospheric scintillation. As DM technology has advanced and evolved, it has found applications in a variety of optical systems that require precision control of an optical surface.

Xinetics personnel have been involved with DMs since the early developments of the first deformable mirrors. To date AOA-Xinetics has delivered more than 400 DMs for various applications including atmospheric compensation, laser communications, directed energy and high contrast imaging for ExoPlanet detection and characterization. New applications for DMs include Ophthalmology and X-ray optics.

Each application has its own set of requirements, but all applications require precision control of the optical surface. In the following sections we address the deformable mirror technologies, design considerations, and applications for X-ray test facilities and X-ray telescopes for astronomical applications

2. DEFORMABLE MIRROR TECHNOLOGIES

2.1 Actuator Materials

AOA-Xinetics normally uses Lead Magnesium Niobate (PMN) electrostrictive[1] actuators to adjust the figure their deformable mirrors[2]. This relaxor ferroelectric ceramic material[3] is usually chosen over piezoelectric materials such as Lead Zirconate Titanate (PZT)[4] for it's excellent dimensional stability, repeatability, reliability, high speed operation capability, and ability to be tailored to optimize displacement and hysteresis over the desired operating temperature range. The CTE of PMN is closely matched to the CTE of Silicon mirror substrates for ultimate thermal stability; its

quadratic response (non-linear) is highly linear within its (normal) ± 30 Volt operating range; and the high modulus of PMN produces optimal stiffness for Surface parallel Actuated (SPA) DMs. Figure 1a shows the transfer function and the creep and hysteresis performance of PMN compared to PZT, while Figure 1b shows how actuator materials can be tailored to optimize performance over a desired operating temperature range.

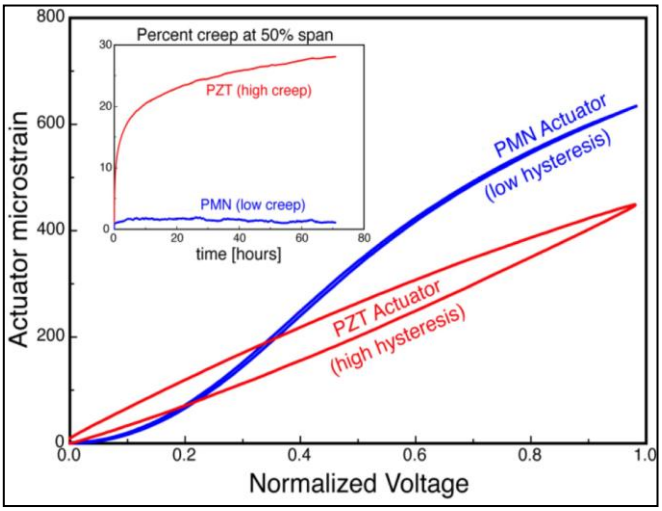

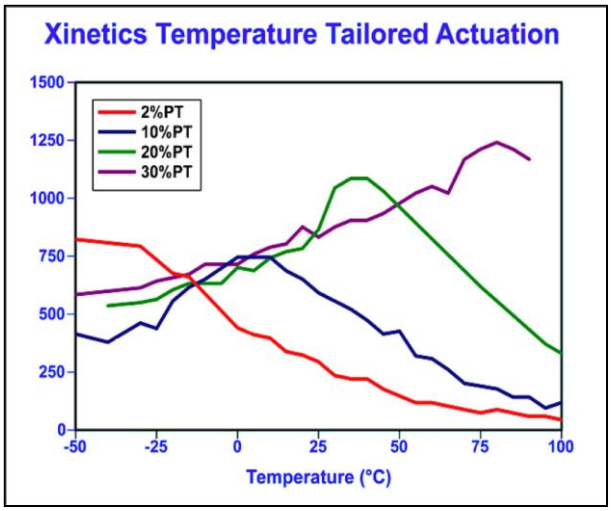

Figure 1. The creep and hysteresis performance of PMN and PZT actuators (on the left), and the effect of dopants on the actuator performance as a function of temperature (on the right).

2.2 Deformable Mirror Architecture

Traditional deformable mirrors[5] (Figure 2) consisted of 37 to 941discrete PMN actuators with 5 to 9 mm spacing and ~4 microns of stroke; a continuous facesheet of ULE or single crystal Silicon with apertures up to 30 cm, 5%-10% inter-actuator coupling with inter-actuator stroke limited to ½ free stroke; and a rigid reaction structure of the same material as the facesheet (to minimize thermal distortions) athermally bonded to mounting structure.

These DM's, designed to correct for atmospheric scintillation, had a high bandwidth with an actuator rise time of 100μs (99% settled), >4 kHz small signal bandwidth which produced 8kHz full stroke bandwidth. The optical surface of these DMs was typically ¼ wave PV, 1/20 wave rms with a surface roughness <20 Å rms (5 Å rms was achievable) and an optical coating of protected silver, aluminum, gold, or multi-layer dielectric.

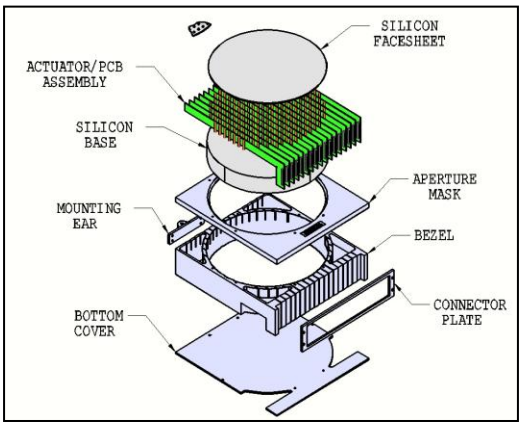

Figure 2. Traditional Deformable Mirror architecture

2.3 DM Design Considerations

Optimized DM designs[6] are based on actuator and facesheet trades. Actuator considerations include (1) the number of actuators, which determines the spatial frequency correctability; (2) actuator spacing, which determines the size of the mirror and the influence function; (3) the stroke range which determines the wavelength and magnitude of surface figure errors; and (4) the type of actuator, which determines the voltage range, power dissipation, actuator hysteresis, aging and creep, and repeatability, aging and life. Of course, the slew rate of the electronics that drive these actuators must have the temporal frequency response and closed loop bandwidth to support the particular application.

Configuration considerations include (1) the influence function shape, which is determined by the facesheet thickness, actuator spacing and the actuator stiffness and force; (2) the thermal environment and load, which determines the facesheet material (ULE or Silicon) and the optical coating; and (3) the natural resonant frequency, which determines the DM's dynamic response.

Optical Figure considerations include (1) the optical quality of the DM, which depends on the facesheet material and polishing pressure; and (2) the mirror's reflectivity which depends on the ability to deposit the desired optical coating, which depends on the deposition temperature required for the coating. Figure 3 shows the results for a typical design trade that assumed an actuator stress of 1000 MPa, PP stress of 2000 MPa, actuator coupling of 10% and optical ripple of 10 nm rms.

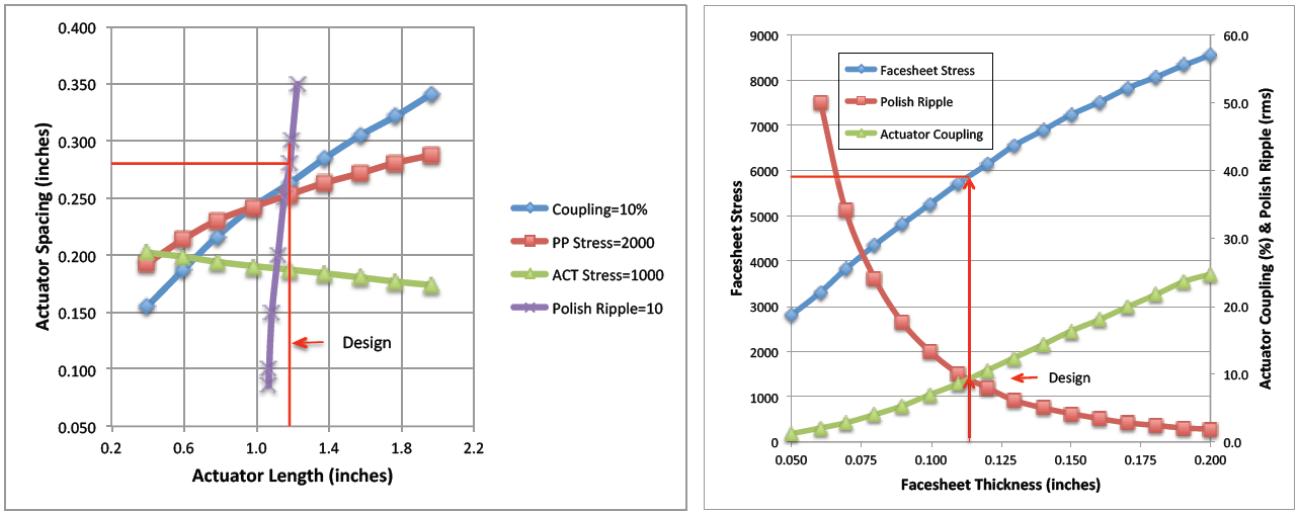

Figure 3. The results of a DM design trade for the PMN actuator length (1.18 inches, 30 mm) and spacing (0.28 inches, 7 mm) on the left, and the optimum Silicon facesheet thickness (0.113 inches, 2.9 mm), facesheet stress (5870 MPa), actuator coupling (9.3%), and optical ripple (9.3 nm rms) on the right.

2.4 Advanced Deformable Mirrors

The number of wave front fluctuations that a DM can correct is proportional to the number of actuators, or degrees of freedom that can be controlled. Although correction for low spatial frequency errors in the wavefront provides the most significant improvement in image quality, correction for mid-spatial frequency errors is essential for achieving the highest image quality. In particular, high contrast imaging for astronomical applications demands the highest possible actuator density to achieve the 10^{-9} to 10^{-10} contrast ratios required for Exoplanet detection and characterization[7]. Higher actuator density comes at the expense of smaller, more closely packed influence functions and decreased amplitude error correction capability (stroke), however; which led Xinetics to develop surface parallel actuation techniques.

Figure 4 illustrates the path that advanced DM development has taken at AOA-Xinetics[8]. Surface normal actuation was added to surface parallel actuation; and Xinetics' family of discrete actuators with 5 to 9 mm spacing was joined by actuator arrays with spacing as small as 1 mm.

Surface Parallel Actuation (SPA) provides many significant advantages over Surface Normal Actuation (SNA): (1) it provides figure control without the requirement for a reaction mass or stiff back structure; (2) the actuators can be imbedded directly into the ribs of an open back mirror or bonded directly to the back of a facesheet, providing compact, ultra-lightweight mirrors; and (3) the actuators can be used individually with a small stroke to correct

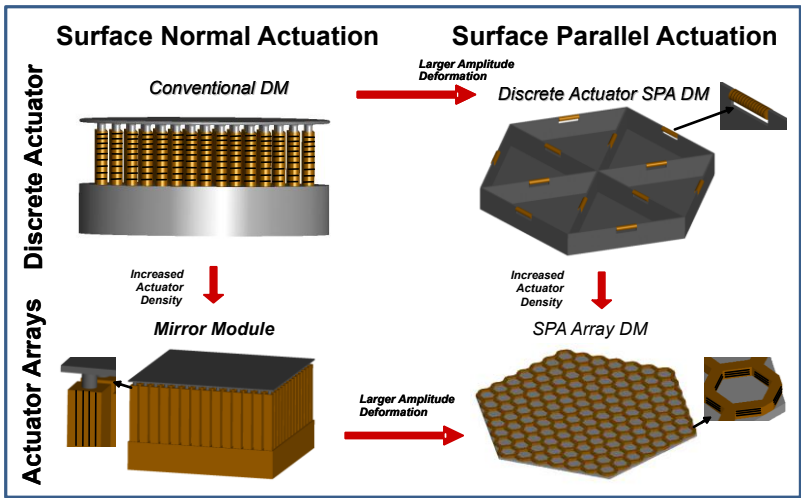

Figure 4. The evolution of DM technology at Xinetics from surface normal actuation to surface parallel actuation, and from discrete actuators to actuator arrays.

high spatial frequency surface figure errors, or ganged to together to provide a very large stroke to correct low spatial frequency errors. Figure 5 shows the performance of AOA-Xinetics 420 channel Photonex SPA DM. It has a monolithic array of hexagonal actuators with 4 mm spacing that provide an individual actuator stroke of 477 nm, and global influence function with all actuators working together to provide a total stroke of 42 microns.

The DM can be flattened to 8 nm rms, and has excellent correctability for low order Zernike polynomials. It has a high bandwidth with an actuator rise time of 100μs (99%settled) that provides >8kHz small signal bandwidth. The optical surface figure is ¼ wave rms unpowered, with surface roughness < 5 Å. The mirror coating can be protected silver, aluminum, gold or a multilayer dielectric.

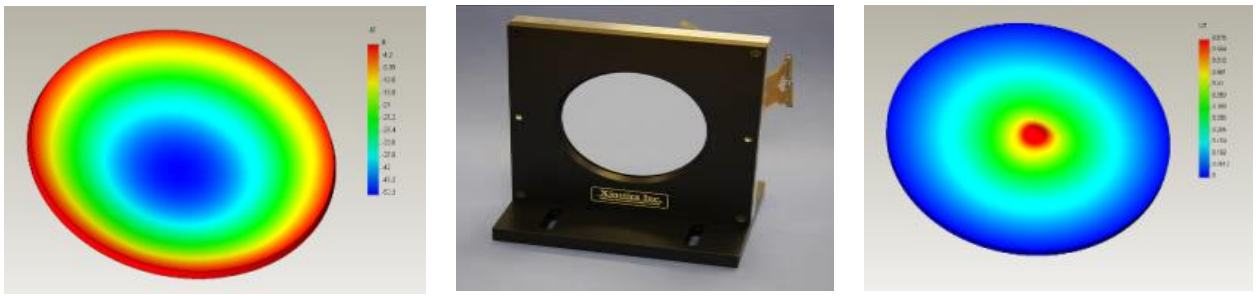

Figure 5. AOA-Xinetics' Photonex 420 Channel DM has a monolithic array of actuators with 4 mm spacing and a 100 mm aperture. It combines large amplitude and high spatial frequency correction capability.

Modular arrays of surface normal actuators have also provided a dramatic improvement in performance for conventional DMs. DM's fabricated with 32 x 32 actuator arrays with 1 mm spacing have demonstrated 0.25 Angstrom precision in correcting wavefront errors in the High-Contrast Imaging Testbed (HCIT)[9] at JPL with no change in their figure when unpowered for more than a month. AOA-Xinetics product line now includes (Figure 6) conventional SNA DMs with discrete actuators, SNA Module DMs, and SPA DMs.

Figure 6. AOA-Xinetics' Product Line includes surface normal actuated mirrors with discrete actuators and modular actuator arrays as well as surface parallel actuated mirrors with planar actuator arrays.

3. X-RAY OPTICS APPLICATIONS

Since 2008 AOA-Xinetics has been pursuing the application of its deformable mirror technologies to adaptive grazing incidence grazing optics for X-ray space telescopes and ground based X-ray test facilities, including synchrotron X-ray beam lines. This effort began when Northrop Grumman was partnered with scientists at the Smithsonian Astrophysics Observatory (SAO) to study the Generation-X mission[10], one of the studies funded by NASA to provide an input to the

National Research Council's 2010 Decadal Survey of Astronomy and Astrophysics[11]. That effort was followed by the development of a pair of Kirkpatrick-Baez mirrors for use in the X-ray test facility at the University of Colorado's Center for Astrophysics and Space Astronomy (CASA). More recently, AOA-Xinetics has been studying to the application of their DM technologies to optics for synchrotron beam lines.

3.1 Generation-X

Generation-X (Gen-X) will be an extremely powerful X-ray observatory with 5 times better spatial resolution, 1200 time larger collecting area, and 30,000 times greater point source sensitivity than the Chandra X-ray Observatory currently operating in High Earth Orbit. The Gen-X mission concept was originally developed in 2006 to 2007 as one of NASA's Vision Mission studies intended to lead to a new start in the next decade. It was further developed in 2008-2009 by one of NASA's Advanced Strategic Mission Concept Studies (ASMCS). The Gen-X Mission Parameters from the ASMCS study are listed in Table 1.

Table 1. Generation-X Mission Parameters

Effective Area (1 keV)	50 m^2
Angular Resolution (HPD)	0.1 arcsec
Field of View (radius)	5 arcmin
Spectral Resolving Power	1,000-10,000
Background (0.1 - 2 keV)	0.004 ct $ksec^{-1}$ $arcsec^{-2}$
Energy Band	01. - 10 keV
Launch Vehicle and Orbit	Ares V to L2
Launch Date	2025-2030

Chandra's X-ray telescope has 4 nested cylindrical grazing incidence Wolter Type 1 mirror pairs ranging from 0.6 m to 1.2 m in diameter with a 1 keV effective area of 0.04 m^2. Gen-X will achieve the required collecting area by an order of magnitude increase in the mirror diameter, and populating it with several hundred nested primary and secondary mirror shells, each of which must be as thin as possible to meet the mirror's 12,500 kg mass limit. Slumped glass shells as thin as ~0.2 mm have been fabricated at Goddard Space Flight Center for the NUSTAR and future X-ray missions[12], and have been baselined for Gen-X. . Each shell would be made up of mirror segments 1 m long by 1 m wide or wider. Each nested shell requires precision alignment into the supporting structure. Electrostrictive or piezoelectric actuators located at fixed radial mounting points would micro-adjust radial position, primary to secondary alignment as well as tip and tilt.

A substantial improvement to the Gen-X mirror figure quality over current capability will be required, however, particularly at low spatial frequency, to achieve 0.1 arc-sec angular resolution. The Gen-X scientists at SAO[13] suggested this improvement could be achieved by using planar PZT actuators attached to the mirror in a unimorph topology to "adjust" the optical figure to obtain the desired shape. The selection of the active optics approach must be chosen so that it not only improves mirror figure but also can be incorporated into the mirror without adding substantial thickness or structure that would obscure the path of X-rays within the annular gap between adjacent nested mirrors.

Figure 7 shows the shows the Power Spectral Density (PSD) requirements for the Gen-X mission before and after figure correction, as well as the predicted performance for the mirrors using Xinetics actuators. The figure also shows the performance achieved for Chandra, the requirements for the Constellation-X mission, and the requirements for a mirror for the Department of Energy's National Ignition Facility (NIF).

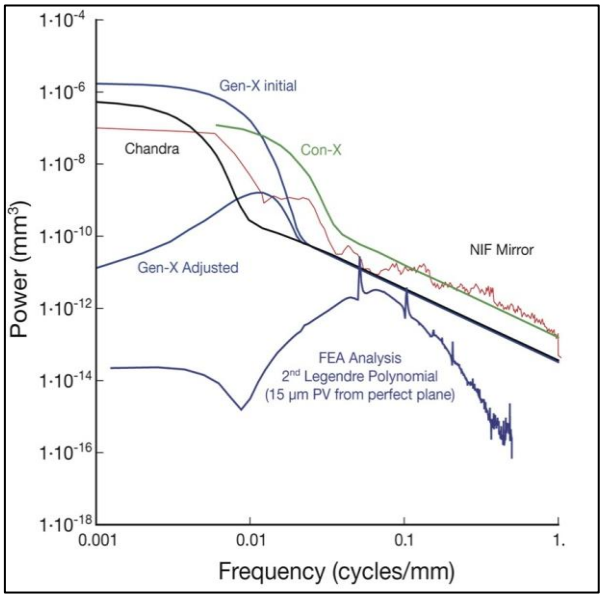

Figure 7. The PSD requirements for the Gen-X mirrors before and after adjustment, plus the predicted performance for the Gen-X mirrors after adjustment with Xinetics PMN SPA actuator arrav.

AOA-Xinetics approach to meeting these requirements[14] was to bond a planar array of SPA actuators to the mirror shells with an actuation spacing of about 15 mm, providing an areal density slightly less than 6000 actuation sites per m^2. Actuators would be fabricated with Xinetics standard process: thin layers of PMN tape cast ceramics are co-fired into planar arrays to produce SPA actuators. The ground electrodes are continuous within the sheet but the signal

electrodes are discrete to a particular region and can be independently addressed. After firing, the modules are machined, bonded to the substrate and electrodes are attached. The planar geometry of the arrays permits a wide variety of geometric electrode patterns that can be tailored for a particular optical application. Because the arrays are on the backside of the mirror and depending on nested mirror spacing, do not add substantially to obscuration.

A finite element model 1 m long by 0.1 m wide was built in order to simulate the performance of these mirrors. The width of the model was selected to economize computer resources and run times. The model had 623 actuators with approximately 8 actuators across the width, giving good figure control along the center of the panel in the axial direction, the primary figure of merit we were trying to achieve relative to Gen-X. The FEA model and typical influence functions from various actuation sites within the model are shown in Figure 8. There are two characteristics of the influence functions that are worth mentioning. First, there is localized bending at the actuation site which is to be expected providing good high spatial frequency figure control. But more important for the Gen-X application is the long tails of the influence functions that provide good surface deflection as well as smooth summing over large distances and large numbers of actuators. Because of the large deflection that can be achieved with SPA actuation, we performed our modeling by assuming that the initial mirror surface was a perfect plane. The plane was then deformed to meet both the axial and circumferential figure requirements for the outermost Gen-X mirror. The nominal axial radius of curvature is nearly 8000 m providing a sag from plane of only 15 microns; the circumferential radius of curvature is much less at 7.86 m, producing a much greater sag.

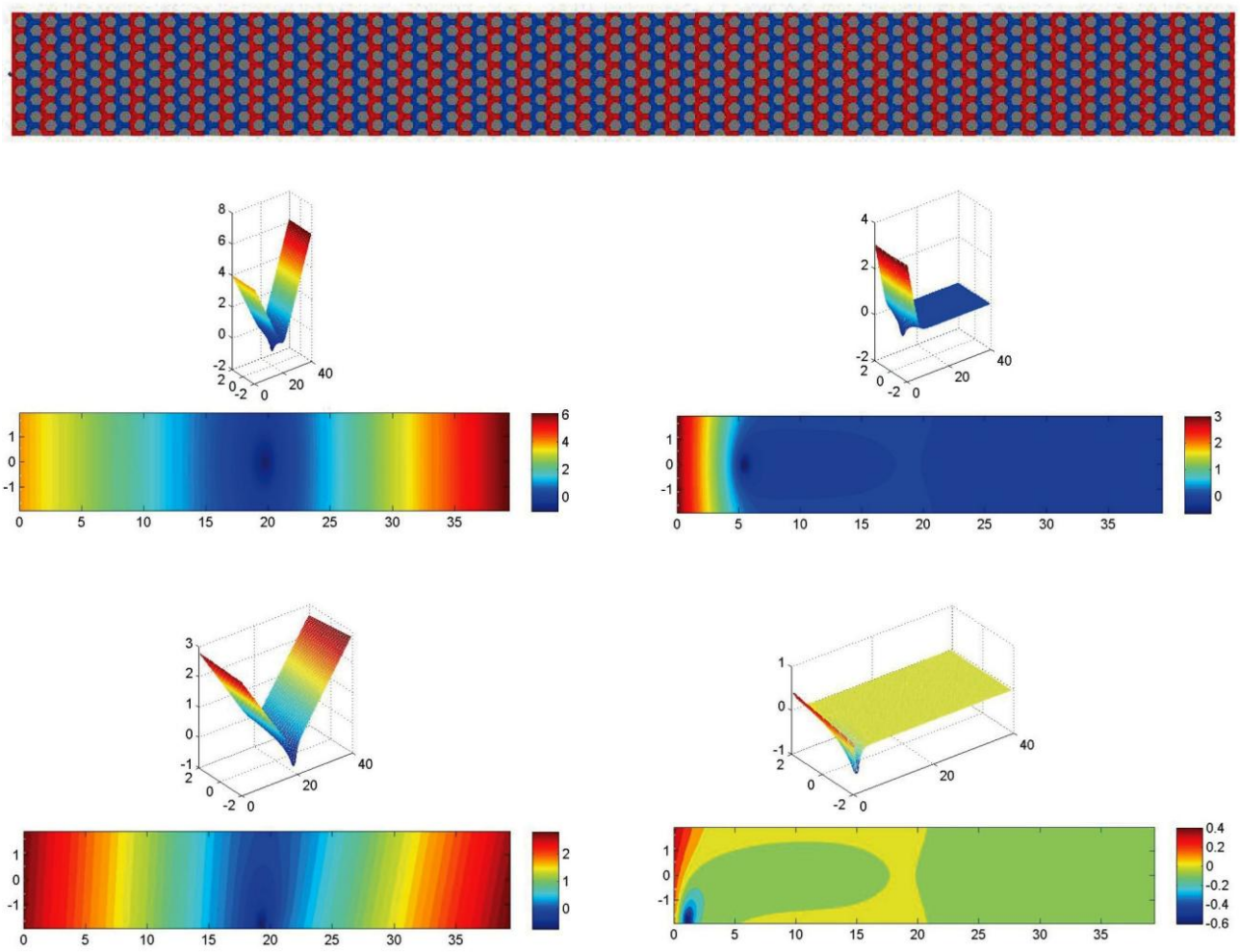

Figure 8. The Gen-X mirror FEA Model and typical influence functions from various actuation sites within the model.

Figure 9 shows residual error plots generated from our finite element modeling. We first analyzed for bending the plane to match the outermost primary reflector prescription in the axial direction. We used a 2nd order Legendre polynomial

(parabola) having the same axial sag as the Gen-X prescription to simplify analysis rather than the exact prescription. This captures the main low spatial frequency shape of interest. This is the most important criterion for obtaining the 0.1 arc-second resolution goal of Gen-X. The residual error of the entire surface was 40Å rms. This is below the 65Å rms error requirements over the spatial frequency bandwidth of 0.001 to 0.01 mm^{-1} suggested by Reid et al.[13]. It should be noted that this error is over the entire surface and includes the ripple evident at the free edges of the model. The model was exercised in the free condition without regard for any edge supports. Furthermore, no modeling was done to optimize the actuator layout by merging the array to tighter spacing at the edges to minimize these errors. To estimate the best that one might achieve if edge effects were reduced to that of the center section, we selected only those points that made up the center half of the strip and also removed about 4mm from the inlet and exiting "lip" of the reflector. This reduced the error to 28 Å PV and 5.5 Å rms. A second analysis was performed in which the planar model was deformed to match both the axial figure requirement and the circumferential radius of the reflector. In this case the edge ripple increased and the whole surface PV increased to 20,250 Å and 2,620 Å respectively. Selecting the center strip and eliminating the inner and exiting lip as was done previously reduced these to 1,970 Å and 376 Å respectively. While the actuators may have sufficient authority to bend a plane to the desired shape circumferentially, the residual error is too great and necessitates starting with a petal close to the desired figure. Later analyses performed during the design and fabrication of KB mirrors for the Colorado test facilities showed that the errors at the edge of the mirrors could be greatly reduced by using much smaller actuators at the edge of the petals.

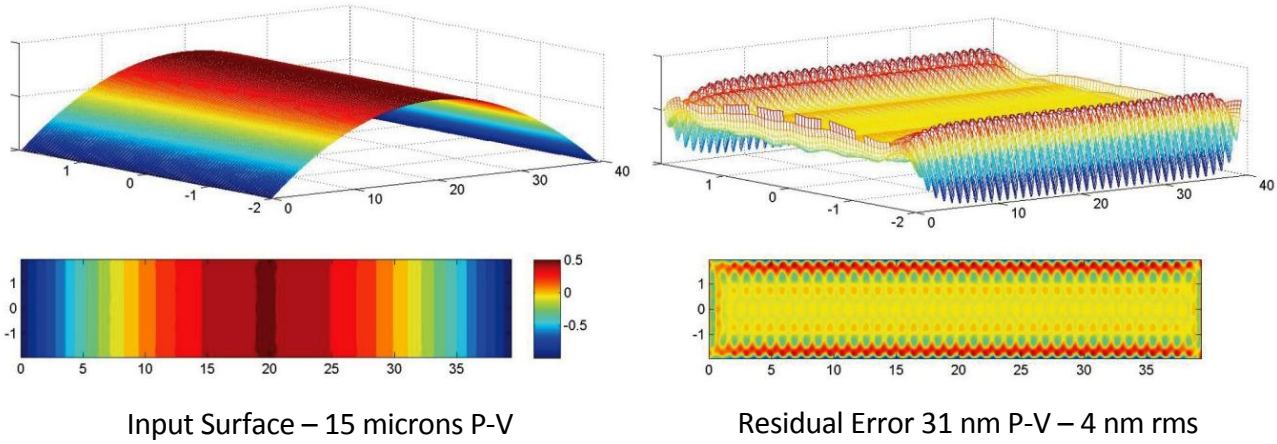

Figure 9. Residual error from actuating a plane surface to the axial figure of one of the primary mirror reflectors of the Generation-X design concept.

3.2 Kirkpatrick-Baez (KB) Mirrors

After we completed our ASMCS effort we initiated an Internal Research & Development (IR&D) project to develop a mirror that could demonstrate the use of Xinetics SPA technology for X-ray adaptive optics. Working with personnel from the University of Colorado's Center for Astrophysics and Space Astronomy (CASA) we designed, fabricated and tested a pair of KB mirrors that could replace the existing spherical KB mirrors in CASA's vacuum test facility. Figure 10 shows the KB mirror location in the test chamber located in the Astronomical Research Laboratory (ARL) at CASA that has been set up to measure the performance of off-plane gratings for high resolution X-ray spectroscopy from sounding rocket and space satellites.

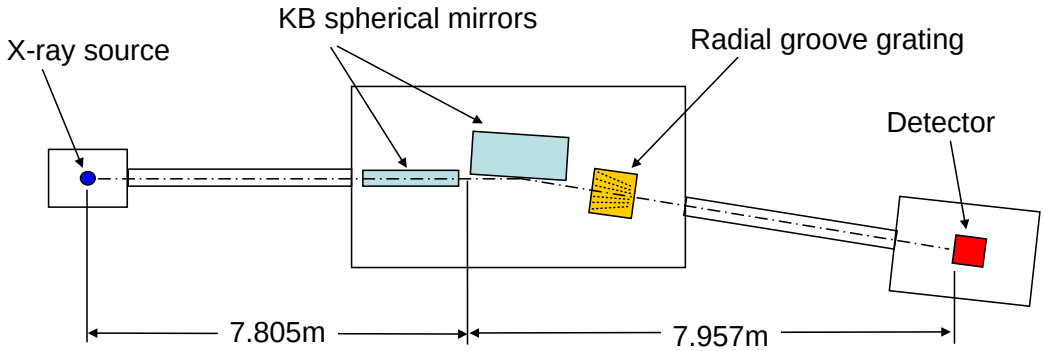

Figure 10. KB mirror location in the CASA/ARL vacuum test facility configured to test off-plane grating efficiency and resolution.

Figure 11 shows the actuator layout for AOA-Xinetics' KB grazing incidence X-ray mirrors in the CASA/ARL vacuum test facility. Table 2 lists the KB mirrors properties used for their design

Table 2. KB Mirror Properties

Parameter	Facesheet	Actuators
Material	Silicon	PMN
E (psi)	1.90E+07	1.52E+07
Nu	0.26	0.33
Density (lb/in^3)	0.084	0.276
CTE (K^{-1})	2.621E-06	1.0E-06
Length (cm)	30	1
Width (cm)	10	2
Thickness (cm)	0.254	1.27
Quantity	1	108

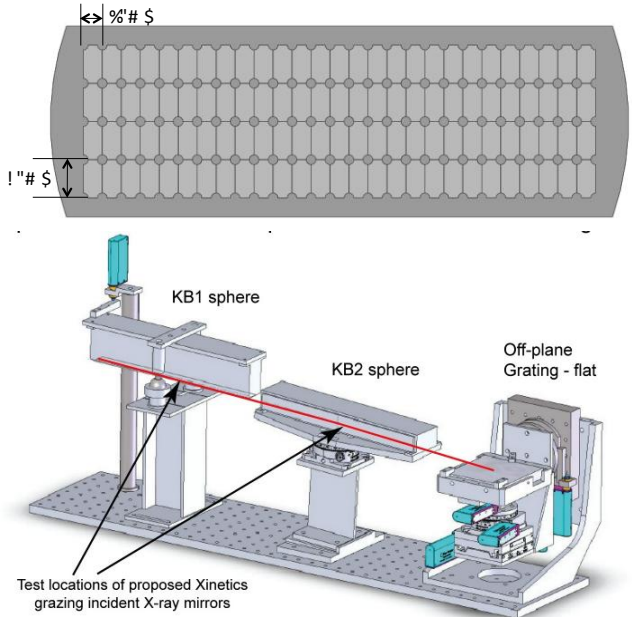

Figure 11. The actuator layout on the Xinetics' KB mirror substrate, and the proposed location for the Xinetics mirrors in the CASA/ARL vacuum test facility.

The mirror substrate is the best 4-inch wide section machined out of a 12-inch diameter optical quality silicon wafer. The substrate was then sent to a vendor who coated it with Platinum.

Three planar SPA actuator arrays, each with a 4 x 9 array of 1 cm x 2 cm PMN actuators, were fabricated to provide an 8 cm x 27 cm actively controlled mirror area. After the actuators were electrically connected and tested, they were bonded to the back of the substrate. A 50 Volt bias was applied to the actuators while the epoxy was curing so the actuators could be both expanded and contracted to control the mirror figure.

The mirror was then attached to its 4.5 x 13 x o.25-inch 6061 Aluminum mounting plate with a 0.4 –in long stainless steel flexure at each corner of the substrate. Slots were cut in in the plate for a 51-pin connector for each 36-actuator array. The AL plate was then attached to a delta-plate with a high precision Newport screw at each corner for tip/tilt control. This mirror mounting approach is shown in Figure 12, along with a picture of Xinetics' first Kirkpatrick-Baez mirror.

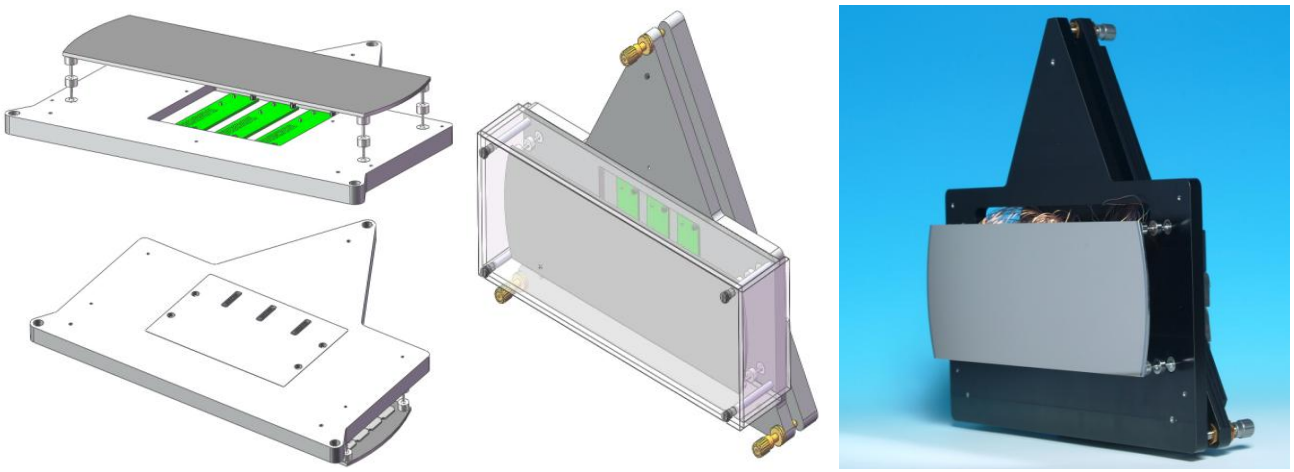

Figure 12. The KB mirror mounting approach and Xinetics' first Kirkpatrick-Baez grazing incidence X-ray mirror.

Table 3. KB Mirror Optical Test Data

KB Mirror Test Data (Tip/Tilt and Piston removed)	Mirror #1		Mirror #2	
	P-V (μm)	μm rms	P-V (μm)	mm rms
Average 20 Volt Deta IF's	2.7854	0.4556	2.4496	0.3956
Average 30 Volt Deta IF's	3.7095	0.6022	2.3839	0.3834
Full (12 x 4 -in) aperture w/48V bias	7.342	1.142	10.565	2.093
Active (27x8-cm) aperture w/48V bias	4.381	0.677	6.88	1.437
Active Aperture w/ mirror flattened	0.757	0.033	0.725	0.067
Improvement Factor	5.8	20.5	9.5	21.4

The KB mirrors' performance was tested at Xinetics using their Generation III drive electronics and a 12-inch Zygo with 640x480 pixel resolution. 20 V and 30 Volt delta influence functions were first collected for each of the 108 actuators by applying ±10 and ±15 Volts from the 50V bias. These influence functions were then used with a least squares solution to command the mirror to its best, flattest figure. Finally, starting from the flattest figure, the mirror surface was commanded into was commanded to several levels of cylinder (up to the Zygo capture limit). The results of the optical influence function measurements and figure flattening tests are shown in Table 3. Figure 13 shows the results for one of commanding the mirror to a cylindrical shape with a 500-m radius. Note, the residual surface figure errors are concentrated at the corners and edges of the mirror and the center section that reflects the (3mm diameter) X-ray beam is 100's of times smoother as shown in Figure 14. Similarly, commanding the mirror to correct a P-V=14.511μ and STD=3.329μ leaves a residual surface with P-V=1.596μ and STD=0.115μ. The central 27x3 centimeter section of mirror's 27x8 cm active area has a P-V=0.911μ and STD=0.0638μ, a factor of 2 better.

There are a number of lessons to be learned from this IR&D Project: (1) the overall P-V and STD values for adaptive X-ray mirrors are dominated by surface figure errors at the edges and support points; (2) the central regions of the mirrors are far better corrected; (3) the optical quality of the mirror substrate ultimately limits the performance of the mirror, so it must be of the highest possible quality (within budget constraints); (4) square actuators layouts are better than hexagonal actuator for the best edge correctability; (5) better edge control can be achieved by having smaller, denser arrays of actuators at the edge than in the central region of the mirror; and (6) pre-figuring the mirror substrate (and actuator arrays) to the approximate figure of the actuated mirror minimizes the stroke requirements of the actuators and preserves the stroke for higher spatial frequency error correction.

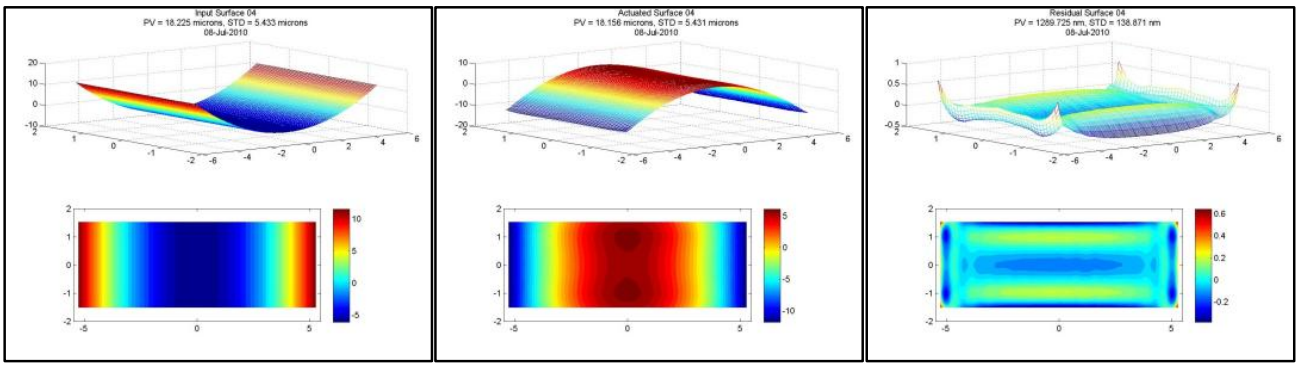

Figure 13. A KB mirror commanded to a cylindrical shape with a radius of curvature of 500 meters. The input surface (left) has a P-V=18.225μ and STD=5.433μ while the actuated surface (center) has a P-V=18.156μ and STD=5.431μ which leaves a residual surface figure with P-V=1.290μ and STD=0.139μ (concentrated at the edges and the corners)

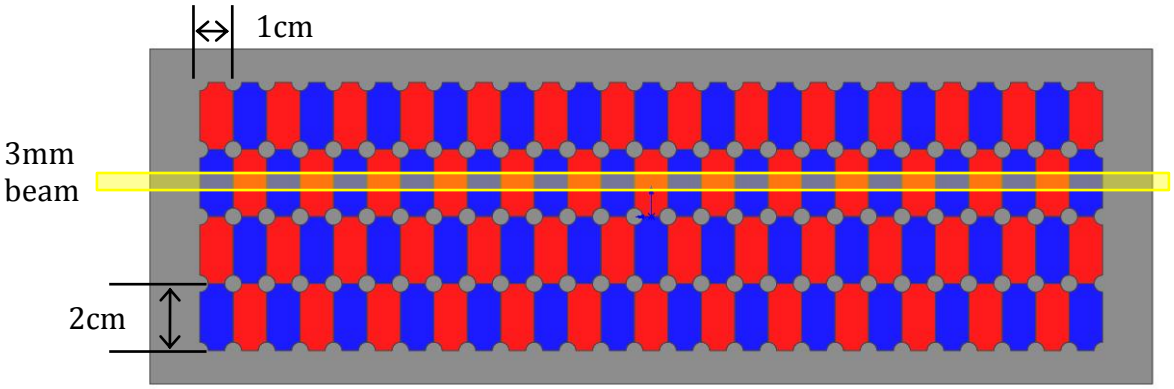

Figure 14. A 3 mm X-ray beam centered on actuators near the center of the mirror shown in Figure 13 is reflected by a well-corrected surface with a P-V=1.362 nm and 0.228 nm

3.3 Bendable Mirrors for Synchrotron Beamlines

Most recently AOA-Xinetics has been looking at the use of adaptive grazing incidence optics in synchrotron X-ray beamlines to provide real-time, closed loop feedback control to maintain beam quality despite mirror temperature changes and other temporal and transient effects. Adaptive optics would also enable the beam to be directed at different targets without breaking vacuum. PMN actuators are extremely good temperature sensors; so adaptive optics can also be "smart mirrors", measuring and correcting themselves for changes in mirror temperature. "Peak-up" algorithms have also been developed for adaptive optics, enabling the actuators to be "dithered" to find the optimum setting to correct for wavefront errors throughout the beamlines' entire optical system to minimize the beam spot size and maximize the energy deposited on the target.

In order to assess the performance of PMN actuators bonded to a typical beamline mirror, we built a finite element model of a planar 100 x 10 x 5 cm silicon mirror with a 3-point kinematic mount and 500 of our KB mirror's 1x2 cm actuators bonded to the rear surface in a 5 x 100 actuator array, as shown in Figure 15. We then used this model to evaluate the actuators to bend this mirror into a cylindrical shape.

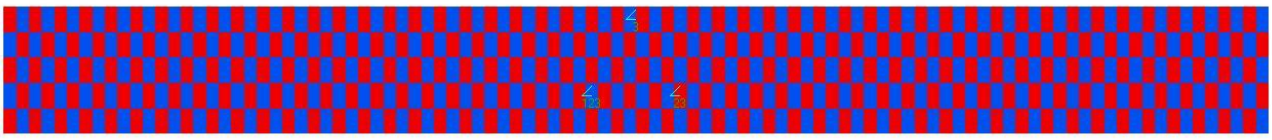

Figure 15. The actuator layout for the FEA model of a 100 x 10 x 5 cm thick adaptive Silicon mirror for a synchrotron X-ray beamline.

As expected, the model showed that as mirror thickness increase the Influence Function (IF) becomes broader and its amplitude decreases (figure 16). Thus mirrors with thinner substrates can correct higher amplitude and higher spatial frequency distortions.

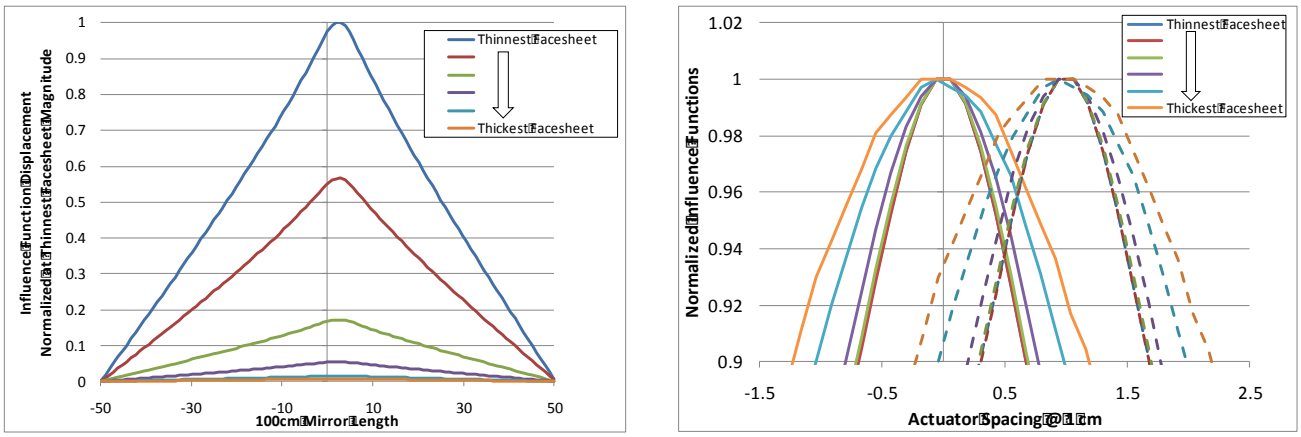

Figure 16. Influence Function (IF) trends as a function of mirror substrate thickness show the IFs width is directly proportional, and its amplitude is inversely proportional, to substrate thickness.

This effect is clearly shown in Figure 17. With one actuator across the full 100cm the amplitude is maximized, but only half a cycle can be corrected. At the other extreme, with 100 1cm actuators, many cycles are possible across the full 100cm but at a cost of amplitude; and the maximum amplitude decreases with the correction for higher spatial frequency errors.

Figure 18 shows a full excursion of the mirror. 100 ppm of full actuation equates to 30 microns of cylinder distortion. Subtracting out the pure cylinder, the residual surface has P-V=0.3028μ and STD=0.0947μ for 98.956% correctability. Correcting 2.5 microns of cylinder for a 100 x 8 cm strip in the middle of the mirror reduces the residual surface figure errors to P-V=0.0043μ and STD=0.0004μ.

Clearly, minimizing the required figure corrections produces the best surface quality, which reinforces the argument for pre-figuring the mirror substrates to the shape desired during operation.

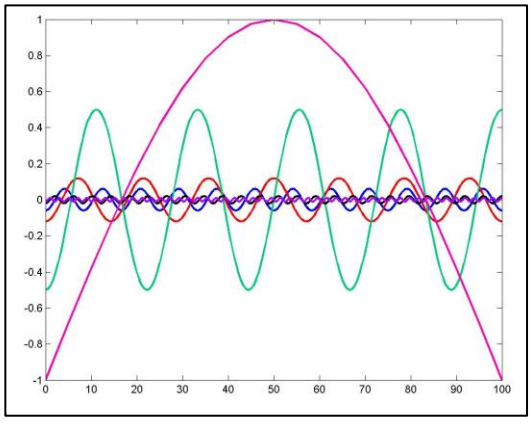

Figure 17. Larger actuators yield higher amplitudes at lower spatial frequencies, while higher actuator areal densities enable high spatial frequency error correction.

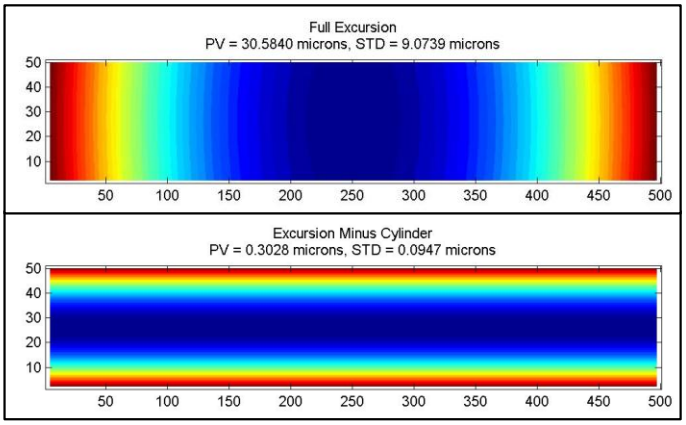

Figure 18. Full excursion of the 100 x 10 cm mirror actuators produces 30 microns of cylinder with residual surface of 300nm P-V and 95 nm rms

4. SUMMARY

AOA-Xinetics has been the world leader in the development of adaptive optics for wavefront error correction for more than 25 years, and has delivered more than 400 deformable mirrors for various applications including atmospheric compensation, laser communications, directed energy and high contrast imaging. They are continuing to improve and mature conventional actuator and DM technology, to invent new architectures with unique characteristics to expand DM performance and applicability, and to apply actuator and DM technology to new applications that enable game-changing optical systems.

Their technology innovations include the development of monolithic actuator modules for SNA DM with up to 9,216 actuators with 1 mm spacing, hybrid active SIC mirror technology for large, lightweight segmented mirrors with replicated nanolaminate optical surfaces; SPA DMs that combine large amplitude and high spatial frequency correction in a compact lightweight package; and Integrated Wavefront Corrector Mirrors that combine wavefront control with beam steering functionality in single component.

Since 2008 AOA-Xinetics has been pursuing the development of adaptive grazing incidence optics for X-ray applications, including X-ray telescope for future space observatories, adaptive mirrors for ground based X-ray test facilities and synchrotron beamlines. Their research indicates adaptive X-ray optics can meet the stringent requirements for the next generation of X-ray telescopes and can provide useful new capabilities for ground based X-ray test facilities.

5. ACKNOWLEDGEMENTS

We acknowledge helpful discussions with Dan Schwartz, Paul Reid and Roger Brissenden at SAO regarding development of adaptive optics for the Generation-X mission and other future X-ray observatories.

REFERENCES

[1] http://en.wikipedia.org/wiki/Electrostriction
[2] http://www.as.northropgrumman.com/businessventures/aoa-xin/deformable_mirrors/index.html
[3] http://guava.physics.uiuc.edu/~nigel/courses/563/Essays_2005/PDF/delgado.pdf
[4] http://en.wikipedia.org/wiki/Lead_zirconate_titanate
[5] Wellman, J. A., Price, T. R., and Cavaco, J. L., "Traditional deformable mirror technology and applications," Proc. SPIE 7803-10 (2010).
[6] http://en.wikipedia.org/wiki/Deformable_mirror
[7] Trauger, J.T., and Traub, W. T., "A laboratory demonstration of the capability to image an Earth-like extrasolar planet," Nature 446, 771-773 (2007)
[8] Wellman, J. A., Cavaco, J. L., and Pearson, D. D., "Advanced deformable mirror technology and applications," Proc. SPIE 7803-14 (2010).
[9] Sidick, E., Kuhnert, A. C., and Trauger, J.T., "Broadband performance of TPF's High Contrast Imaging Testbed: Modeling and Simulations," Proc. SPIE 6306-32 (2006).
[10] Wolk, S. J., et al., "Science with Generation-X," Proc. SPIE 7011 701130 (2008).
[11] National Research Council Committee for a Decadal Survey of Astronomy and Astrophysics, "New Worlds, New Horizons in Astronomy and Astrophysics," National Academies Press. ISBN 978-0-309-15796-4 (2010).
[12] Zhang, W., et al., "Development of X-Ray Reflectors for the Constellation-X Observatory", SPIE Proc., vol. 5168, 168 (2004).
[13] Reid, P., et al., "Constellation-X to Generation-X: Evolution of large collecting area, moderate resolution grazing incidence x-ray telescopes to larger area, high resolution, adjustable optics" Proc. SPIE 5488, 325 (2004).
[14] Lillie, C., Pearson, D., Plinta, A., Metro, B., Lintz, E., Shropshire, D. and Danner, R., "Adaptive grazing incidence optics for the next generation of x-ray observatories," Proc. SPIE 7803, 78030Q (2010).